Modification of Turbulent Flow using Distributed Suction

Maurizio Quadrio[1,*], J.M.Floryan[2], Paolo Luchini[3]

[1] *Dept. Aerospace Engineering, Politecnico di Milano, Italy*
[2] *Dept. Mechanical and Materials Engineering, University of Western Ontario, Ontario, Canada*
[3] *Dept. Mechanical Engineering, University of Salerno, Italy*

Email: *maurizio.quadrio@polimi.it, luchini@unisa.it, mfloryan@uwo.ca*

ABSTRACT

The long-term objective of this investigation is the development of techniques for re-arrangement and control of turbulent flows by using a suitably roughened wall. As a preliminary step towards this goal, we describe in the present paper the analysis of the turbulent flow in a plane channel modified by a sinusoidal distribution of suction/blowing at the wall with zero net mass flux. The tool by which the whole investigation is carried out is the Direct Numerical Simulation (DNS) of the incompressible Navier–Stokes equations.

The fundamental result of this preliminary study is that the suction wavelength has a dramatic effect on the modification induced on the turbulent flow by the suction at the wall. Large wavelengths produce very high increases in the friction drag, whereas smaller wavelengths can lead to a friction decrease up to 4-5%.

1 INTRODUCTION AND MOTIVATION

The technological relevance and the scientific interest of the studies aimed at controlling turbulent flows are today widely recognized [1]. A detailed knowledge of the turbulence-producing cycle taking place in the near-wall region of a wall-bounded shear flow is a preliminary step towards the ability of controlling the flow itself. The control is typically focused towards one of the two classical objectives of reducing the friction drag and increasing the turbulent mixing. In §2 we review briefly the techniques currently discussed in the literature for the control of wall turbulent flow. Most often they rely on external energy input (active techniques), and/or are based on non-trivial control laws (closed-loop techniques), requiring a distributed array of a large number of sensors and actuators, thus increasing the difficulties for a practical realization.

A passive, open-loop strategy which has not received much attention to date is the use of non-planar surfaces. The only such example is the use of riblets [2], small-scale V-grooves aligned in the streamwise direction, which can produce up to 8-10% reductions in friction drag. Besides of that, the effects of the shape of the rigid wall have not been investigated in great detail. There are indeed quite a few papers related to the turbulent flow over a sinusoidal wavy wall, but a systematic analysis of all the parameters of the sinousoidal corrugation has never been performed, and the focus has never been the modification of the drag or mixing properties of the flow.

The turbulent flow over a wavy wall is interesting *per se*. In the recent literature, evidence of large-scale streamwise Taylor-Görtler-type vortices is found in the experimental analysis by Gschwind, Regele and Kottke [3], but on a wavy channel with such a large ratio of wave amplitude and channel height to make it essentially a quasi-planar flow problem with mild streamwise curvature. Some large-scale streamwise vortical structures, in the range of parameters where curvature effects are comparable to those considered in the present work, have been found by Gong, Taylor and Dörnbrack [4] and recently confirmed by Günther and Rudolph von Rohr [5]. In their experiment, carried out with a wavelength λ of the corrugation equal to the full height $2h$ of the channel, and with a peak-to-peak distance of 10% of the wavelength, they found with a Proper Orthogonal Decomposition of the velocity fluctuations that the dominant eigenmodes possess a characteristic spanwise scale of $3h$, and are consistent with the existence of streamwise-oriented large-scale

*Visiting Professor, Dept. of Mechanical and Materials Engineering, University of Western Ontario

vortical structures. They state that the only parameter which characterizes the flow, besides the Reynolds number based on the channel heigth, is the ratio of roughness wavelength and wave amplitude, thus not attributing any importance to the absolute value of the wavelength. The very presence of longitudinal vortices is still a discussed issue. It can be explained with a Craik-Leibovich type-2 (CL2) instability, as described in [6], but can be explained also by centrifugal effects due to a Görtler-type instability. The last mechanism cannot be ruled out at the present state of our knowledge.

The turbulent boundary layer over a wavy wall has been studied by Hanratty and coworkers at University of Illinois, both in experiments and DNS, for many years. For example [7] contains an exhaustive investigation made with DNS of the turbulent flow over a wavy wall with wavelength $\lambda = 2h$, replicating a similar experimental analysis described in [8]. Another DNS-based numerical study by De Angelis, Lombardi and Banerjee is reported in [9]: $\lambda = 1.04h$ and $\lambda = 2.09h$ were considered.

The flow over a wavy wall has been extensively studied in the *laminar* flow regime. Floryan and coworkers [10] [11] have found with a linear stability analysis that a two-dimensional, sinusoidal waviness of the wall described in terms of a single Fourier mode in the streamwise direction can affect the stability properties of the laminar flow in a significant way. They found a range of corrugation wavelengths, bounded from above and from below, where a new type of instability, due to centrifugal effects, determines the appearance of streamwise vortices, arranged in the spanwise direction with a preferred wavelength. This conclusion has been reached for both Couette and Poiseuille flows.

It is not clear however how these results (and the results from the CL2 instability mechanism) apply to the turbulent flow in a wavy channel. This is the main motivation of this paper. We want to investigate whether the sensitivity of laminar flow to wall waviness (and in particular to its wavelength) can be found also in turbulent flows.

In this preliminary stage of the research, we study through a number of Direct Numerical Simulations the properties of the turbulent channel flow over a simulated two-dimensional distributed surface roughness, obtained through a sinusoidal distribution of blowing/suction velocities in the wall-normal direction, with a zero net mass flux. The equivalence between a wavy wall and a sinusoidal distribution of suction velocity at a planar wall still has to be proven; nevertheless Floryan [12] found that the mechanisms governing the transition process are qualitatively similar. A qualitative relationship between the suction distribution and the equivalent waviness of the wall is shown in Fig.1, together with the relative origin of the streamwise coordinate: $x = 0$ denotes the position where the blowing velocity is maximum, and corresponds to one quarter of wavelength of the sinusoidal solid wall starting from a crest.

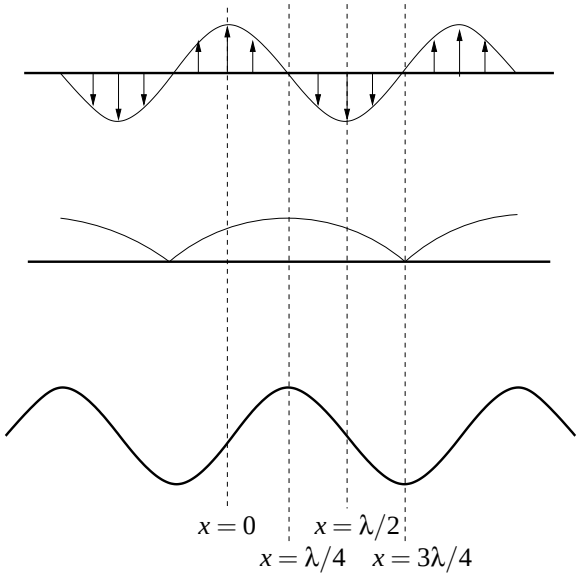

Figure 1: Equivalence between distributed suction over a flat wall (top), the corresponding streamfunction of the flow modification (middle) and the equivalent sinusoidal wall (bottom).

The structure of the paper is as follows. First in §2 a brief overview of the available techniques for the control of turbulent flow will be given. In §3 the numerical method and the computer code used for the simulations are described. §4 illustrates the discretization and the suction parameters used in the simulations. In §5 we report results concerning the modification of the mean friction through sinusoidal blowing. In §6 we report some turbulent statistics, first in §6.1 averaged over the whole channel and then in §6.2 as a function of the streamwise position over the suction distribution. Lastly, §7 is devoted to the Conclusions.

2 CONTROL OF TURBULENT FLOWS

In recent years, the improvement in our knowledge of turbulence, and the very possibility offered by MEMSs to achieve a fine-scale distribution of sensors and actuators [13] has boosted the number of studies related to turbulence control and drag reduction. Following the

use of riblets and the injection (in liquid flows) of long-chain polymeric molecules, several attempts to control a turbulent wall flow by employing a number of different techniques are reported in the recent literature. Virtually all of them are in the proof-of-principle stage, and the tool used for developing and testing the control strategies is most often the Direct Numerical Simulation (DNS) of the incompressible Navier–Stokes equations. Thanks to this research tool, different various ideas can be tested in a cheap and cost-effective manner, and even unphysical simulations can be carried out, to the aim of gaining additional insight into the real physics of the flow [14].

Recently developed control techniques span from the use of spanwise oscillation of the wall [15], [16], to the use of a spanwise-oriented oscillating Lorentz force [17] or a spanwise travelling wave [18]. All these techniques are *open-loop*, since they do not require feedback in the control law. Other, more complex *closed-loop* control strategies can be devised where a feedback is exploited in the control law. We mention in this category the so-called opposition control through a distributed array of sensors (in the interior of the channel) and actuators (local, instantaneous blowing/suction at the wall), introduced by Choi, Moin and Kim [19], and the wall vorticity flux control by Koumoutsakos [20], that uses the same type of actuators but relies only on information available at the wall. An additional class of active, closed-loop control systems is growing, which can be broadly classified as optimal (or suboptimal) controls. They employ concepts from control theory [21], and in particular one promising approach exploits the power of adjoint operators, computing the Fréchet derivative of a cost function to optimize friction drag. Some examples are described in [22], [23] and [24].

It is clear however that passive, open-loop techniques (like riblets) are best suited for practical implementations: they do not require sensors or actuators and control law, nor they depend on external energy input to function. This is the reason why we focus in the following on relatively simple shape modifications of a planar rigid surface, and in particular on their modeling through a distributed suction.

3 THE NUMERICAL METHOD

The DNS code used in this paper is a parallel solver of the Navier–Stokes equations for an incompressible fluid, a description of which can be found in [25]. It is based on a mixed discretization: Fourier modes are used for the wall-parallel directions, and high-order finite differences in the wall-normal direction. Finite differences are produced from fourth-order accurate, compact schemes acting on a five-point computational molecule in a variable-spacing mesh.

The Navier–Stokes equations are formulated, following a procedure described in [26], in terms of a scalar equation for the normal component of velocity and a scalar equation for the normal component of vorticity, thus achieving the highest computational efficiency when a Fourier discretization is adopted for the homogeneous directions. The non-linear terms of the equations are computed with a pseudo-spectral approach, transforming the flow variables from Fourier space into physical space before computing the products, and taking advantage of computationally efficient Fast-Fourier-Transforms algorithms. Dealiasing in the homogeneous directions is performed by expanding the number of Fourier modes by a factor of at least $3/2$ before going from the Fourier space into the physical space, to avoid the introduction of spurious energy from the high-frequency into the low-frequency modes during the calculations.

The advancement in time of the solution is realized by a commonly used partially implicit approach: non-linear terms are advanced with an explict scheme (a low-storage, three-substeps, third order Runge-Kutta scheme), and linear terms are advanced with an implicit method (a second order Crank-Nicolson scheme) in order to overcome the stability limitations due to the viscous terms.

The code takes advantage of SMP systems, and can be run in parallel on a set of distributed-memory machines (nodes). Thanks to the use of finite differences for the discretization of the normal direction, the parallel algorithm requires no inter-node communication as far as the computation of the explicit convective part is concerned. When data are stored in wall-parallel slices, Fourier transforms are in fact executed in wall-parallel planes. The evaluation of wall-normal derivatives can be done without communication as well, at the expense of duplicating in each machine the four boundary planes shared with the two neighboring nodes. Only the numerical solution of the linear systems arising from the discretization of the implicit part requires some communication, but the impact of the communication time on the overall computing time decreases when the problem size increases, and calculations never happen to be communication-bound.

Our parallel algorithm is suited to a very simple ring topology, schematically illustrated in Fig.2, for the connection of the computing nodes: each machine is directly connected to the previous machine and to the next only, and contains a slice of the computational

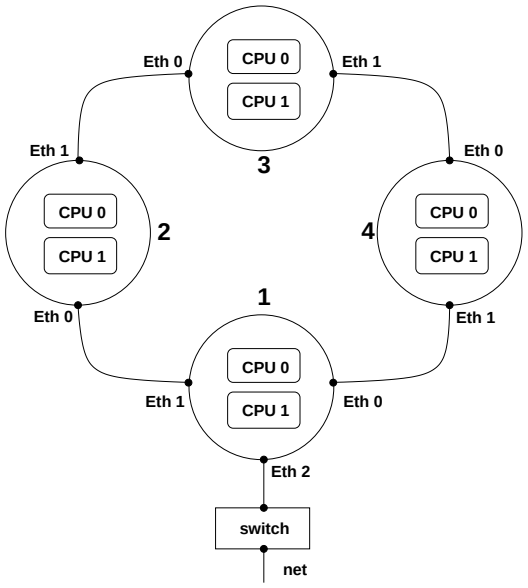

Figure 2: Logical arrangement of 4 computing nodes in a ring connection topology.

domain in the wall-normal direction. The necessity of a hub or switch between computing machines is thus eliminated, increasing simplicity, communication bandwidth, and cost-effectiveness at the same time. The transposition of the flow field between computing nodes is never required, thanks to the design of the parallel algorithm. The code can be run with the highest efficiency on dedicated machines with a connection topology following the logical scheme of Fig.2: see again [25] and [27] for a description of such a machine. The simulations described in this paper have been however performed using a standard cluster of Itanium2 computers, available at the SHARCNET.

4 COMPUTATIONAL PARAMETERS

The simulations described in the following have been carried out for a value of the Reynolds number, based on h, half the channel height, and U_P, the centerline velocity of a laminar Poiseuille flow with the same flow rate, of $Re_P = 4250$. This corresponds to a value of the Reynolds number based on the friction velocity of $Re_\tau = 180$; the centerline velocity is $U_c = 0.78 U_P$. In the simulations the flow rate is kept fixed at a value which is $4/3$ in these units. The computational domain has a streamwise length of $L_x = 2.66\pi h$ and a spanwise width $L_z = 2\pi h$. 129 Fourier modes are used to expand the flow variables in the homogeneous directions, so that the spatial resolution is $\Delta x^+ = 11.7$ and $\Delta z^+ = 8.8$ (quantities indicated with the + superscript are made non-dimensional with the friction velocity and the kinematic viscosity of the fluid). In the wall-normal direction 129 collocation points are used, with a non uniform spacing from $\Delta y^+ = 0.75$ near the wall to $\Delta y^+ = 4.8$ at the channel centreline. For increasing time accuracy, the time step for the temporal integration is set at $\Delta t^+ \approx 0.2$, significantly lower than the stability limit of the time integration scheme.

The suction has been accounted for through the wall boundary condition for the wall-normal velocity component v:

$$v(x, y = 0, z, t) = A \sin(\alpha_s x)$$

where A is the maximum amplitude of the suction distribution, and α_s is the suction wavenumber. The blowing/suction distribution has a zero net mass flux over the entire wall, is stationary in time, costant in spanwise direction and has a sinusoidal variation along the streamwise coordinate, with a wavelength $\lambda_s = 2\pi/\alpha_s$. An identical boundary condition is imposed on the opposite wall at $y = 2h$.

The simulations have been started from a fully developed turbulent flow field computed with a previous simulation with suction turned off, and various combinations of A and α_s have been experimented. Most of the simulations have been run for a total integration time of $500 h/U_P$; the time evolution of selected quantities, notably the two components of the space-averaged friction over the two walls, has been recorded runtime. When turbulence statistics are computed, flow fields are stored on disk during the calculations for later postprocessing: a complete flow field is written to disk every $25 h/U_P$, so that we typically average over 20 well separated flow fields. In addition data from the two walls are averaged together to double the statistical sample.

4.1 Initial choice of the suction parameters

We start our analysis from a laminar calculation, similar to those described in [11] and [10], but using the turbulent mean velocity profile as the base flow. A disturbance in the form of a sinusoidal, two-dimensional blowing/suction distribution of wavelength $2\pi/\alpha_s$ and maximum intensity A is applied at the two walls of a plane flow, and the growth rate of the most unstable disturbance is computed for Reynolds number of $Re = 3000$ based on the channel half-width and the maximum centerline velocity. The base flow coincides with the turbulent longitudinal mean velocity profile previously computed with a DNS at the same Reynolds

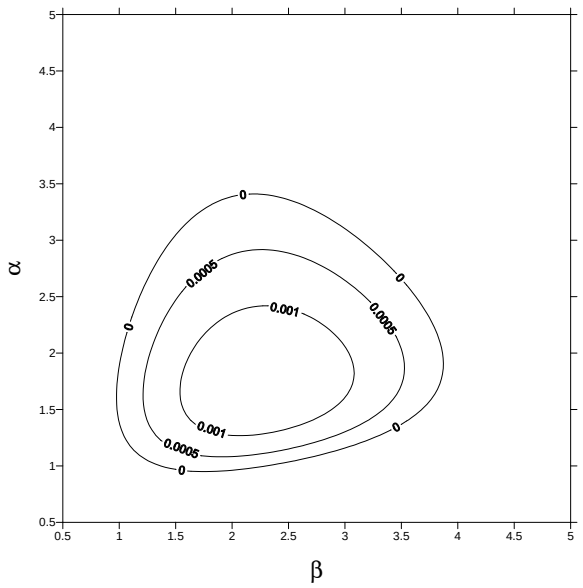

Figure 3: Amplification rate Imag(σ) of disturbances in the form of streamwise vortices as a function of the suction wavenumber α_s and the vortex vawenumber β, with $Re = 3300$ and $A = 0.004$.

number. Disturbances to the base flow have the form:

$$v(x,y,z,t) = \sum_{m=-\infty}^{+\infty} V_m(y) e^{i(m\alpha_s x + \mu z - \sigma t)}$$

where v is one component of the disturbance vector, $V(y)$ is a corresponding function of the wall-normal coordinate only, z is the spanwise coordinate and μ accounts for the periodicity of the streamwise vortices. σ is a purely imaginary number, and describes the growth ($\sigma > 0$) or the decay ($\sigma < 0$) of the perturbations.

A typical result is illustrated in Fig. 3 for a suction amplitude of $A = 0.004$: the neutral curve $\sigma = 0$ encloses a region where σ is positive. This defines a range of suction wavenumbers α_s where centrifugal instability is active, and a corresponding range of spanwise wavenumbers. The most amplified streamwise vortex occurs in this particular case for $\alpha_s = 1.8$ and has a typical spanwise wavenumber of $\beta = 2 - 2.5$.

Such results give us an initial guess for the range of interesting suction wavenumbers, even if we expected only a qualitative guidance.

5 FRICTION

Table 1 reports the time average of the friction coefficient C_f, defined as:

Case	$\alpha_s h$	A/U_P	$10^3 C_f$	%
0	0	0	8.22	0.0
1	0.75	0.08	40.06	387.2
2	0.75	0.04	26.66	224.2
3	0.75	0.02	16.84	104.8
4	0.75	0.01	11.39	38.5
5	0.75	0.005	9.06	10.2
6	0.75	0.002	8.35	1.5
7	1.5	0.08	20.10	144.4
8	1.5	0.04	17.76	115.9
9	1.5	0.02	12.29	49.4
10	1.5	0.01	9.14	11.2
11	1.5	0.005	8.39	2.0
12	1.5	0.002	8.20	-0.3
13	3	0.04	9.24	12.3
14	3	0.02	8.13	-1.1
15	3	0.01	8.09	-1.6
16	4.5	0.08	8.06	-2.0
17	4.5	0.04	7.97	-3.0
18	4.5	0.03	7.86	-4.4
19	4.5	0.02	7.91	-3.8
20	4.5	0.01	8.05	-2.1
21	4.5	0.005	8.15	-1.0
22	6.75	0.08	8.16	-0.7
23	6.75	0.04	8.05	-2.1
24	6.75	0.02	7.99	-2.8
25	6.75	0.01	8.11	-1.3

Table 1: Change in friction coefficient induced by different combinations of the suction amplitude A and the suction wavenumber α_s.

$$C_f = \frac{2\tau_x}{\rho U_b^2}$$

where τ_x is the streamwise component of the shear stress at the wall, and U_b is the bulk velocity of the flow. The computed value of $8.22 \cdot 10^{-3}$ in the case without suction compares very well with the value obtained by [26] in the DNS of a turbulent channel flow at the same Reynolds number, with a difference of 0.4% only.

Observing the results of Table 1 in terms of percentage variations of the friction coefficient allows one to draw two interesting observations. Not only the suction wavenumber has a strong effect on the measured variation of C_f, but the sign itself of the variation is affected: we go from significant friction increases for low wavenumbers to small drag reductions at higher wavenumbers. Although rather low, these drag reduction amounts are above the statistical uncertainty of the data. The maximum drag reduction measured in these preliminary experiments is 4.4%, even though the pa-

rameter space has not been fully explored yet.

There are to our knowledge no previous available data for friction measurements with distributed non-uniform, sinusoidal suction in a turbulent flow. Even in the qualitatively similar flow over a wavy wall, the roughness wavelength has never been varied in a systematic way. In addition, when the wall is not flat the drag budget becomes more complex, since additional terms arise (form drag) which are responsible for a reduction of the friction drag while the overall drag may increase [9]. This is why the drag reducing effect reported here might not have been noticed at all before.

These data are important, since they show that the wavelength of the roughness (or at least of the suction distribution) is a very important parameter of the flow. This is a reasonable result. The effect of the modulation of the turbulent flow by sinusoidal blowing on friction must be mediated by its interaction with the near-wall turbulent structures, which are typical of the near-wall region [28], and are ultimately responsible for the turbulent friction drag. Hence it is reasonable to expect that the nature of this interaction does depend on the ratio between the wavelength of the waves and the streamwise extension of some typical near-wall structures.

From Table 1 an abrupt change of the response of the flow to the distributed suction can be noted between $\alpha_s h = 1.5$ and $\alpha_s h = 3$. If we take $\alpha_s h = 2.25$ as an intermediate point, this translates into a wavelength of 500 viscous length scales. This is a typical length scale in near-wall turbulence. For example Jiménez and Moin [29] in their Minimum Channel DNSs determined the minimal extent of the computational domain that is needed to sustain the turbulence cycle, speculating that they correspond to the minimal length scales which are relevant to a sustained turbulence and must be represented by the calculations. Even if their study was focused on the precise determination of the minimal width of the computational domain, an estimate for the streamwise wavelength gave $L_x^+ = 400 - 600$. This is approximately the length of the near-wall, quasi-streamwise vortical structures, which are significantly shorter than the low-speed streaks they produce, which extend up to thousands of viscous length units [30].

This length scale can be converted into a time scale by a suitable value of convection velocity. At the wall, velocity fluctuations are convected at a velocity of approximately $10u_\tau$, and this points to a time scale of 50 viscous time units. Quadrio and Luchini [31] recently computed a typical time scale from the statistical observation of the flow in a pseudo-Lagrangian frame that moves so as to maximize the space-time correlation. This time scale quantifies the different life span of the fluctuation of different flow variables, and is 61 viscous time units for the fluctuations of the longitudinal friction.

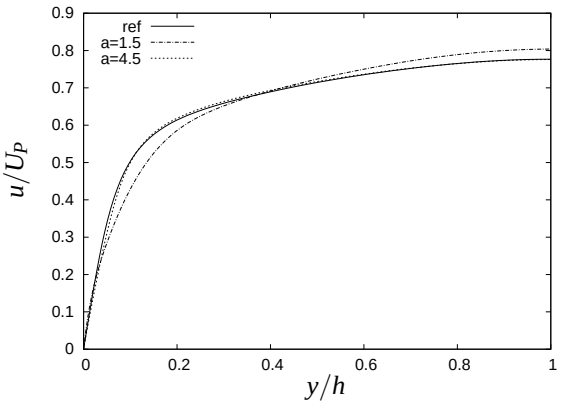

Figure 4: Mean streamwise velocity profile for cases I and II, compared to the reference flow (continuous line).

6 TURBULENCE STATISTICS

In this Section we report some preliminary turbulence statistics. Thanks to the ergodic hypothesis, they are averaged over time and the homogeneous spanwise direction z. Contrarly to the standard channel flow, the streamwise direction x is not homogeneous anymore, and the flow quantities depend on the location over the undulation (or sinusoidal distribution of suction). In §6.1 we report a few quantities averaged also over the entire wavelength, whereas in §6.2 some results collected over different positions along the suction wave are shown. Additional results will be presented at the Conference.

6.1 Averaged statistics

Fig.4 shows the modification induced in the mean velocity profile by the wall suction with amplitude $A = 0.02U_P$, for two cases with $\alpha_s = 1.5$ and $\alpha_s = 4.5$, denoted as case I and case II in the following, and corresponding to a drag increase and a drag reduction respectively. As expected from the observation that the mean friction increases in case I and decreases in case II, the two profiles show an opposite behavior. Case I with longer suction wavelength induces an overall larger velocity in the very near-wall region, then a velocity deficit can be observed for $0.05 < y/h < 0.3$.

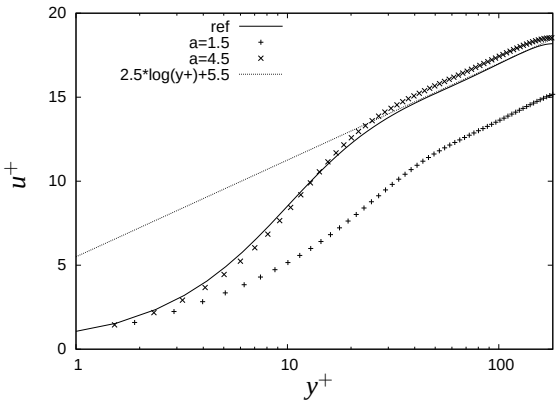

Figure 5: Mean velocity profile plotted in wall units for case I and case II, compared to the reference case (continuous line). Dotted line is the universal law of the wall $u^+ = 2.5 \log y^+ + 5.5$

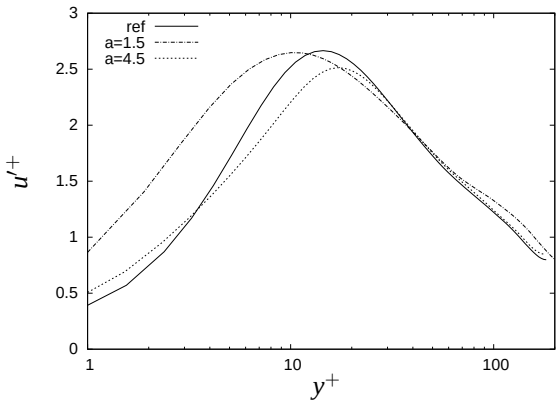

Figure 6: Root-mean-square value of the u velocity fluctuations, averaged over the whole suction distribution: comparison between case I, case II and reference flow.

This velocity deficit has to be compensated for in the outer region, since the calculations are carried out at a constant flow rate. Case II with smaller suction wavelength on the other hand produces smaller effects (barely discernible on this scale), but in the direction of reducing the slope of the velocity profile at the wall.

A better look at the same data can be taken by scaling them with near-wall variables, as shown in Fig.5. Each velocity profile is made nondimensional by means of the friction velocity computed on the basis of the average friction of the corresponding computational case. Case I presents the standard characteristic of a turbulent flow over a rough wall, with a drag increase and a consequent downward shift of the logarithmic portion of the velocity profile. Case II presents a reduced friction drag, with the consequent upward shift. This is a general feature of drag-reducing flows. There is however an important difference with standard flows with drag reduction, which are homogeneous in the streamwise direction. In these cases the mean velocity profile remains uniformly higher than the reference profile for the standard unmanipulated turbulent flow, see for example [16] for the drag-reducing flow over an oscillating wall. Here we can observe the presence of a near-wall region, extending approximately for the extent of the viscous sublayer, where, as a consequence on the local non-equilibrium due to the streamwise variations, the velocity profile with suction attains smaller values. We recall however that this profile is the result of an average over the entire wavelength.

In Fig. 6 we report the root-mean-square values of the fluctuations for the longitudinal velocity distribution, averaged over the whole wavelength, as a function of the distance from the wall. The actual friction velocity is used. The results are consistent with the previous observations. In absolute values case I shows significant changes which extend to a significant portion of the channel, but these changes are absorbed by the nondimensionalization with the actual friction velocity. A generalized increase of the fluctuations in the near-wall region can be observed regardless of the adopted discretization. The peak value is essentially unchanged. Case II on the other hand presents smaller modifications limited to $y^+ < 30$, where the fluctuation level decreases, except for the very near-wall region $y^+ < 4$. The peak position is shifted outwards, pointing to an increase of the viscous sublayer thickness, and the peak value is slightly reduced. The outer layer is unchanged when scaled with the proper friction velocity.

6.2 Turbulence statistics at different positions along the wave

The streamwise direction for this flow is not homogeneous, and the flow characteristics depend on the x position over the suction distribution.

We show first in Fig. 7 the mean velocity profile in the near-wall region for case I, at four different streamwise positions over a single suction wavelength. An outer scaling is used, and only the near-wall region is shown. As expected, in the region where the blowing velocity away from the wall is maximum, i.e. $x = 0$, the slope of the mean velocity profile is the lowest. On the other side, where the suction is maximum, the local friction is maximum. The same plot for case II (not shown) has a similar qualitative behavior, but the ob-

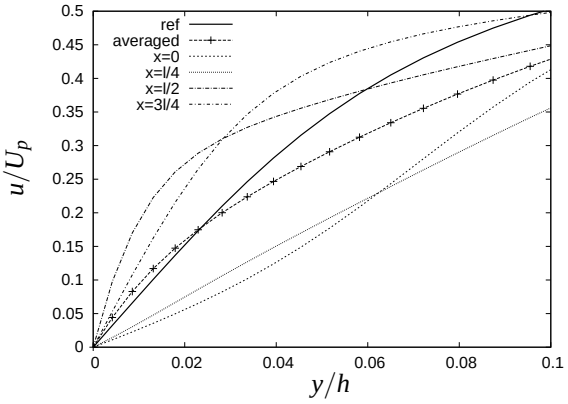

Figure 7: Streamwise mean velocity profile in different positions along the suction distribution: comparison between the wave-averaged profile for case I (line with symbols), and the reference flow (thick continuous line).

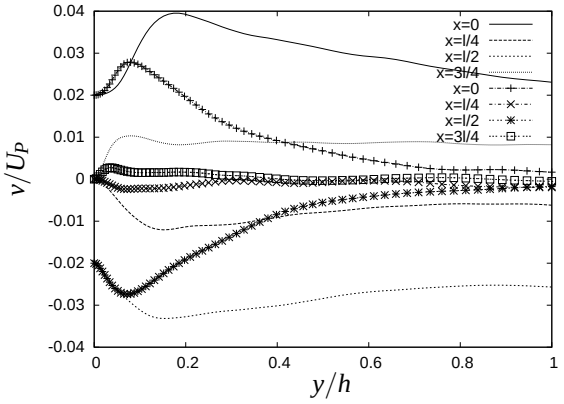

Figure 8: Vertical mean velocity profile in different positions along the suction distribution, case I (lines) and II (lines with symbols) at positions $x = 0$, $x = \lambda/4$, $x = \lambda/2$ and $x = 3\lambda/4$.

served differences are much smaller.

In Fig. 8 the mean profile of the wall-normal velocity component at different locations over the suction distribution is reported. In the standard channel flow this profile is identically zero. Profiles for case I and case II are compared at the same position over the suction wavelength. It can be appreciated how case II, characterized by a shorter wavelength, has a shorter penetration distance into the boundary layer. The wall values at corresponding positions are obviously the same. A distinctive feature is the peak far from the wall at $x = 0$ which is present in both cases, with different intensity in different positions. At $x = 0$ for case I the actual peak is at $y^+ \approx 40$, and its value is almost twice the value of the blowing velocity at the wall.

7 Conclusions

The effect of a sinusoidal distribution of suction at the walls of a turbulent channel flow has been examined, by carrying out a number of Direct Numerical Simulations and by systematically changing both the suction intensity and the suction wavelength λ_s. From the preliminary results reported in this paper, a significant effect of the suction wavelength can be noticed. For relatively long suction wavelengths, we find a dramatic increase in the turbulent drag for relatively small values of the maximum velocity at the wall. When the wavelength is decreased below a threshold value, approximately $\lambda_s = 2.5h$, this effect disappears, and an opposite effect takes place: a small but definite reduction of the friction drag is measured.

These results suggest that, contrary to what is generally stated or assumed in most investigations carried out to date for turbulent flows over wavy walls, the wavelength of the waviness is an important parameter of the flow. Moreover, they open interesting perspectives for the closed-loop control of turbulent flows, either with a distributed suction at the wall or by employing sinusoidal wall roughness, the latter being a passive, closed-loop approach.

Acknowledgments

The last two authors have been financially supported by SHARCNET (http://www.sharcnet.ca) through their Senior Visiting Fellowship Program. The authors also whish to acknowledge the use of SHARCNET's computational resources and the assistance of SHARCNET's technical support staff.

References

[1] T. Bewley. Flow Control: New Challenges for a New Renaissance. *Progress in Aerospace Sciences*, 37:21–58, 2001.

[2] D.W. Bechert, M. Bruse, W. Hage, J.G.T. van der Hoeven, and G. Hoppe. Experiments on drag-reducing surfaces and their optimization with an adjustable geometry. *Journal of Fluid Mechanics*, 338:59–87, 1997.

[3] P. Gschwind, P. Regele, and V. Kottke. Sinusoidal Wavy Channel with Taylor-Görtler vortices. *Experimenal Thermal and Fluid Science*, 11:270–275, 1995.

[4] W. Gong, P.A. Taylor, and A. Dörnbrack. Turbulent boundary-layer flow over fixed aerodynamically rough two-dimensional sinusoidal waves. *Journal of Fluid Mechanics*, 312:1–37, 1996.

[5] A. Günther and P. Rudolph von Rohr. Large-scale structures in a developed flow over a wavy wall. *Journal of Fluid Mechanics*, 478:257–285, 2003.

[6] W.R.C. Phillips, Z. Wu, and J.L. Lumley. On the formation of longitudinal vortices in a turbulent boundary layer over wavy terrain. *Journal of Fluid Mechanics*, 326:321–341, 1996.

[7] P. Cherukat, Y. Na, T.J. Hanratty, and J.B. McLaughlin. Direct Numerical Simulation of a Fully Developed Turbulent Flow over a Wavy Wall. *Theoretical and Computational Fluid Dynamics*, 11:109–134, 1998.

[8] J.D. Hudson, L. Dykhno, and T.J. Hanratty. Turbulence production in flow over a wavy wall. *Experiments in Fluids*, 20:257–265, 1996.

[9] V. De Angelis, P. Lombardi, and S. Banerjee. Direct numerical simulation of turbulent flow over a wavy wall. *Physics of Fluids*, 9(8):2429–2442, 1997.

[10] J.M. Floryan. Centrifugal instability of Couette flow over a wavy wall. *Physics of Fluids*, 14(1):312–322, 2002.

[11] A. Cabal, J. Szumbarsky, and J.M. Floryan. Stability of flow in a wavy channel. *Journal of Fluid Mechanics*, 475:191–212, 2002.

[12] J.M. Floryan. Stability of wall-bounded shear layers in the presence of simulated distributed roughness. *Journal of Fluid Mechanics*, 335:29–55, 1997.

[13] C.-M. Ho and Y.-C. Tai. MEMS and fluid flow. *Annual Review of Fluid Mechanics*, 30:579–612, 1998.

[14] P. Moin and K. Mahesh. Direct numerical simulation: A tool in turbulence research. *Annual Review of Fluid Mechanics*, 30:539–578, 1998.

[15] W.J. Jung, N. Mangiavacchi, and R. Akhavan. Suppression of turbulence in wall-bounded flows by high-frequency spanwise oscillations. *Physics of Fluids A*, 4 (8):1605–1607, 1992.

[16] M. Quadrio and S. Sibilla. Numerical simulation of turbulent flow in a pipe oscillating around its axis. *Journal of Fluid Mechanics*, 424:217–241, 2000.

[17] T. W. Berger, J. Kim, C. Lee, and J. Lim. Turbulent boundary layer control utilizing the Lorentz force. *Physics of Fluids*, 12(3):631–649, 2000.

[18] Y. Du, V. Symeonidis, and G. E. Karniadakis. Drag reduction in wall-bounded turbulence via a transverse travelling wave. *Journal of Fluid Mechanics*, 457:1–34, 2002.

[19] H. Choi, P. Moin, and J. Kim. Active turbulence control for drag reduction in wall-bounded flows. *Journal of Fluids Mechanics*, 262:75–110, 1994.

[20] P. Koumoutsakos. Vorticity flux control for a turbulent channel flow. *Physics of Fluids*, 11(2):248–250, 1999.

[21] S.S. Joshy, J.L. Speyer, and J. Kim. A system theory approach to the feedback stabilization of infinitesimal and finite-amplitude perturbations in plane Poiseuille flow. *Journal of Fluids Mechanics*, 332:157–184, 1997.

[22] C. Lee, J. Kim, and H. Choi. Suboptimal control of turbulent channel flow for drag reduction. *Journal of Fluid Mechanics*, 358:245–258, 1998.

[23] T. Bewley, P. Moin, and R. Temam. DNS-based predictive control of turbulence: an optimal benchmark for feedback algorithms. *Journal of Fluid Mechanics*, 447:179–225, 2001.

[24] P. Luchini and M. Quadrio. Adjoint DNS of turbulent channel flow. In *Proc. of the ASME Fluids Engineering Division of Flow Control*, July 2002. Montreal.

[25] M. Quadrio and P. Luchini. A 4th order accurate, parallel numerical method for the direct simulation of turbulence in cartesian and cylindrical geometries. In *Proc. of the XV AIMETA Conf. on Theoretical and Applied Mechanics*, 2001.

[26] J. Kim, P. Moin, and R. Moser. Turbulence statistics in fully developed channel flow at low Reynolds number. *Journal of Fluid Mechanics*, 177:133–166, 1987.

[27] M. Quadrio, P. Luchini, and J.M. Floryan. A Parallel Algorithm for the Direct Numerical Simulation of Turbulent Channel Flow. In *Proc. of the XI Conf. of the CFD Society of Canada*. Vancouver (CAN), May 28-30 2003.

[28] S. K. Robinson. Coherent motions in the turbulent boundary layer. *Annual Review of Fluid Mechanics*, 23:601–639, 1991.

[29] J. Jiménez and P. Moin. The minimal flow unit in near-wall turbulence. *Journal of Fluid Mechanics*, 225:213–240, 1991.

[30] J. Kim and F. Hussain. Propagation velocity of perturbations in turbulent channel flow. *Physics of Fluids A*, 5(3):695–706, 1993.

[31] M. Quadrio and P. Luchini. Integral time-space scales in turbulent wall flows. *Submitted to Physics of Fluids*, 2003.